Thin Solid Films 519 (2011) 4225–4233

Contents lists available at ScienceDirect

Thin Solid Films

journal homepage: www.elsevier.com/locate/tsf

Studies on the effect of solvents on self-assembly of thioctic acid and Mercaptohexanol on gold

Zhiguo Li [a], Tianxing Niu [a], Zhenjiang Zhang [a,b], Guiying Feng [a], Shuping Bi [a,*]

[a] School of Chemistry and Chemical Engineering, State Key Laboratory of Coordination Chemistry of China & Key Laboratory of MOE for Life Science, Nanjing University, Nanjing 210093, China
[b] College of Chemistry, Chemical Engineering and Materials Science, Soochow University, Suzhou 215006, China

ARTICLE INFO

Article history:
Received 13 December 2009
Received in revised form 19 February 2011
Accepted 22 February 2011
Available online 2 March 2011

Keywords:
Thioctic acid
Mercaptohexanol
Parameters of solvent
Self-assembly monolayer
Cyclic voltammetry
Electrochemical impedance spectroscopy

ABSTRACT

In this article we investigated the effect of solvents (CCl_4, CH_3CN, DMF, ethanol, ethanol–H_2O and H_2O) on self-assembly of Thioctic acid (TA) and Mercaptohexanol (MCH) on gold by cyclic voltammetry (*CV*) and electrochemical impedance spectroscopy (*EIS*). Electrochemical characteristics of TA and MCH self-assembled monolayers (SAMs) formed in different solvents were evaluated by inspecting the ions permeability (interfacial capacitance *C* and phase angle $\Phi_{1\ Hz}$) and electron transfer capability (current density difference Δi and charge transfer resistance R_{ct}). Experimental results indicated that the ability of solvents availing the ordering of SAMs was: for TA, CCl_4>ethanol>CH_3CN>ethanol–H_2O>DMF; for MCH, H_2O>ethanol–H_2O≈CCl_4>ethanol≈CH_3CN>DMF. Through relating the *C*, $\Phi_{1\ Hz}$, Δi and R_{ct} of SAMs (TA and MCH) with parameters of solvent (polarity E_T^N, solubility parameter δ and octanol/water partition coefficients logP_{ow}), it was found that solvents with bigger logP_{ow} (smaller E_T^N and δ) availed the ordering of TA-SAMs but the effect of solvents on MCH self-assembly was complex and MCH-SAMs formed in H_2O (the biggest E_T^N, δ and the smallest logP_{ow}) and CCl_4 (the smallest E_T^N, δ and the biggest logP_{ow}) were more ordered than in other solvents.

1. Introduction

Self-assembled monolayers (SAMs) with thiols on gold are the preferred platform for constructing the diversely functional interfaces based on the "bottom-up" principle [1–6]. Qualities of SAMs assembled on gold (e.g. compactness, orientation, permeation and electron transfer) are related to many factors such as solvent, temperature, concentration of thiols, electrode potential and modes of irradiation (microwave, ultrasonic or magnetic field) [7–38]. Solvent plays an important role in self-assembly of thiols on gold and influences the qualities of SAMs formed [7,8,14–38]. However, up to date, effect of solvent on thiols self-assembly on gold is still not well understood [1]. Through reviewing the reports from literature, we find that electrochemically studying the effect of solvent on self-assembly of thiols on gold is few. Recently, we investigate the self-assembly of $C_{12}SH$ on gold in different solvents by cyclic voltammetry (*CV*) and electrochemical impedance spectroscopy (*EIS*) and obtain that quality of SAMs is related to parameters of solvents (E_T^N, δ and logP_{ow}) [7]. Solvents with bigger E_T^N, δ and smaller logP_{ow} produce more ordered $C_{12}SH$-SAMs [7].

Short-chain thiols especially with terminal groups (—COOH and —OH) are widely applied due to the following aspects: (1) terminal groups (—COOH and —OH) of SAMs can bind with other molecules (e.g. metal ions, protein, and enzyme) by electrostatic interaction or covalent bond for studying electron transfer through SAMs or designing diversely functional interfaces [39–41]; (2) ion permeation and electron transfer proceed easily due to the short distance between analyte and electrode surface, which avail to prepare sensor with high sensitivity [41–43]; and (3) thiols are often assembled on gold nanoparticles to form monolayer-protected clusters (MPCs) [44,45]. Investigating the effect of solvents on thiols self-assembly on gold provides a reference for synthesizing the MPCs with the optimal characteristics and understanding the solvation or penetration phenomena of MPCs [44,45]. Thus, it is important to study the effect of solvents on self-assembly of short-chain thiols with terminal groups (—COOH and —OH).

Thioctic acid (TA), a kind of short-chain disulfide with terminal —COOH group (Fig. 1), is often assembled on gold as a base for the interfacial design due to the increasing stability of SAMs with two S—Au bonds [46]. Mercaptohexanol (MCH), a simple alkanethiol with terminal —OH group (Fig. 1), is widely co-assembled with thiol-DNA on gold to reduce the nonspecific adsorption of DNA [47] and increase the hybridization efficiency of DNA sensor [48]. In this article we investigate the effect of solvents (CCl_4, CH_3CN, DMF, ethanol, ethanol–H_2O and H_2O) on the self-assembly of TA and MCH on gold based on the electrochemical parameters (*C*, $\Phi_{1\ Hz}$, Δi and R_{ct}) by *CV* and *EIS*. Relationship of electrochemical parameters of SAMs (TA and MCH) with parameters of solvents (polarity E_T^N, solubility parameter δ, octanol/water partition coefficients logP_{ow}) and the effect of terminal

* Corresponding author. Tel.: +86 25 83594255; fax: +86 25 83317761.
E-mail address: bisp@nju.edu.cn (S. Bi).

0040-6090/$ – see front matter © 2011 Elsevier B.V. All rights reserved.
doi:10.1016/j.tsf.2011.02.065

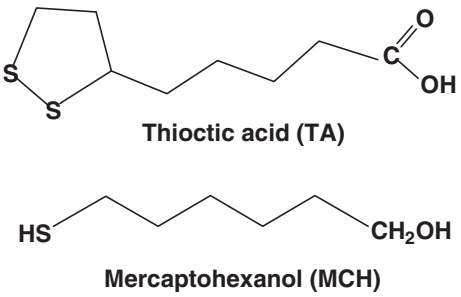

Fig. 1. Molecular structure of Thioctic acid (TA) and Mercaptohexanol (MCH).

groups on thiols self-assembly on gold are discussed combined with the literature report.

2. Experimental procedure

2.1. Chemicals and apparatus

DL-thioctic acid (TA; 98%, Alfa), Mercaptohexanol (MCH; 97%, Aldrich), Sodium sulfate (Na_2SO_4; 99%, Alfa), Potassium hexacyanoferrate (III) ($K_3Fe(CN)_6$; 99%, Sigma), and Ethanol (99.9%, Merck). Tetrachloromethane (CCl_4), Acetonitrile (CH_3CN) and N, N-dimethylformamide (DMF) were of analytical grade from Sinopharm Chemical Reagent Company Ltd., Shanghai. Double-distilled water was used to prepare the aqueous solutions. Electrochemical measurements were performed on a CHI660 (CH Instruments, USA) electrochemical workstation. Equivalent circuit fitting analysis of *EIS* plots was obtained using Zsimpwin software. The fitting curves in the figures were performed using Origin 7.0 (OriginLab Corporation, Northampton, MA). The cell was a three-electrode system with a working electrode of polycrystalline gold electrode (geometric area, 0.0314 cm^2, CH Instruments), a counter electrode of platinum and a reference electrode of saturated calomel electrode (SCE). Solutions were degassed with nitrogen for at least 15 min prior to each experiment and a nitrogen atmosphere was maintained over the solutions. The temperature was kept at 25 ± 1 °C over the course of the experiment with a CS-501SP super digital thermostat bath (Huida Experimental Equipment Ltd., Chongqing, China).

2.2. Pretreatment of gold electrodes

Polycrystalline gold electrodes were hand-polished with microcloth pads and alumina slurries of decreasing particle size (1.0, 0.3 and 0.05 μm), then dipped into newly prepared piranha solution (concentrated H_2SO_4:30% H_2O_2 = 3:1, ratio of vol.) for 2 min. The gold electrodes were then sonicated in double-distilled water for 15 min and electrochemically polished in N_2-purged 0.5 M H_2SO_4 solution from −0.4 to + 1.5 V at 0.1 $V s^{-1}$ until reproducible voltammograms were obtained. Following this, the electrodes were rinsed with double-distilled water and ethanol, then blown to dry with 99.999% highly pure nitrogen. The real surface area of the gold electrodes were determined by integrating the charge of reduction peak of gold, assuming a value of 400 μC cm^{-2} for a monolayer of chemisorbed oxygen on polycrystalline gold [49]. The roughness factor of the gold electrode was found to be 1.5 ± 0.2.

2.3. Preparation of SAMs

The gold electrodes were immersed into 1 mM fresh thiols (TA or MCH) dissolved in different solvents (CCl_4, CH_3CN, DMF, ethanol, ethanol–H_2O (ratio of vol., 1:1) and H_2O) for 24 h self-assembly. Because TA was nearly insoluble in H_2O, we only investigated the self-assembly of MCH on gold in thiols aqueous solution. When the assembly was finished, the gold electrodes were taken out and rinsed with respective solvent and double-distilled water in turn. After this, the electrodes were put into the electrochemical cell for experimentation.

2.4. Electrochemical characterization

The electrochemical characteristics of TA-SAMs and MCH-SAMs were investigated based on the parameters including C, $\Phi_{1\ Hz}$, Δi and R_{ct} from *CV* and *EIS* plots. C, $\Phi_{1\ Hz}$, Δi and R_{ct} had different meanings for characterizing the structure of SAMs [18,50–53]. C showed the average distribution of ions and water in SAMs [51]; $\Phi_{1\ Hz}$ reflected the magnitude of ion permeability in SAMs [18,50]; Δi and R_{ct} were highly sensitive to film defects [51–53].

C was measured from *CV* performed from −200 to +200 mV in 0.1 M Na_2SO_4 solution at different scan rates v (0.1, 1, 5, 50 $V s^{-1}$) based on $C = i/2vA$, where i was the summed current (μA) from the positive and negative scan directions at 0 mV, v was the scan rate ($V s^{-1}$) and A was the real area of the gold electrodes (cm^2) [54,55]. The absolute value of phase angle at 1 Hz ($\Phi_{1\ Hz}$) was used to evaluate the tightness of SAMs [18,50]. The bigger the $\Phi_{1\ Hz}$ was, the tighter were the formed SAMs. $\Phi_{1\ Hz}$ was obtained by impedance analysis at 0 V in 0.1 M Na_2SO_4 blank solutions with frequency ranged from 0.1 Hz to 10^5 Hz and 5 mV amplitude.

CV experiment was performed in 2 mM $K_3Fe(CN)_6$ − 0.1 M Na_2SO_4 aqueous solutions with scan zone from −0.2 to +0.5 V at 0.1 $V s^{-1}$. Current density difference for $Fe(CN)_6^{3-}$ at −0.2 V and 0.5 V ($\Delta i = |i_{-0.2\ V} - i_{+0.5\ V}|$) was used to investigate the electrochemical response of $Fe(CN)_6^{3-}$ (when *CV* of $Fe(CN)_6^{3-}$ presented redox peaks, Δi was the difference of redox peak current density) [7]. Impedance measurement was carried out in 2 mM $K_3Fe(CN)_6$ −0.1 M Na_2SO_4 aqueous solutions with frequency ranging from 0.1 Hz to 10^5 Hz and 5 mV amplitude. The potential was fixed to formal potential $E^{o'}$ (0.18 V). The *EIS* plots were simulated from a Randle equivalent circuit (*RQRW*) (Fig. 2) comprising a parallel combination of constant phase element (*CPE*) represented by Q and a faradaic impedance Z_f in series with the uncompensated solution resistance R_s. The faradaic impedance Z_f was a series combination of charge transfer resistance R_{ct} and the Warburg impedance W [56].

3. Results and discussion

3.1. Electrochemical characteristics of TA-SAMs and MCH-SAMs on gold assembled in different solvents

We investigated the characteristics of TA-SAMs and MCH-SAMs on gold assembled in different solvents by *CV* and *EIS* (Fig. 3 and Table 1).

3.1.1. TA-SAMs

Fig. 3(A, B, C, D) showed the *CV* and *EIS* plots of bare Au and TA-SAMs. Charging current of TA-SAMs formed in CCl_4 was the smallest and in DMF the biggest (Fig. 3A). This indicated that TA-SAMs formed in CCl_4 were the most ordered, whereas TA-SAMs formed in DMF were highly disordered. Correspondingly, $\Phi_{1\ Hz}$ of TA-SAMs formed in CCl_4 was the biggest (86 ± 2^o) and the smallest (82 ± 2^o) in DMF (Fig. 3B). Fig. 3C and Fig. 3D showed that TA-SAMs formed in CCl_4 baffled electron transfer of $Fe(CN)_6^{3-}$ the biggest with Δi (22 ± 1 μA cm^{-2})

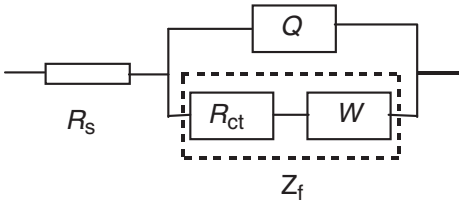

Fig. 2. The equivalent circuit for simulating EIS plots performed in 2 mM $Fe(CN)_6^{3-}$–0.1 M Na_2SO_4 solution.

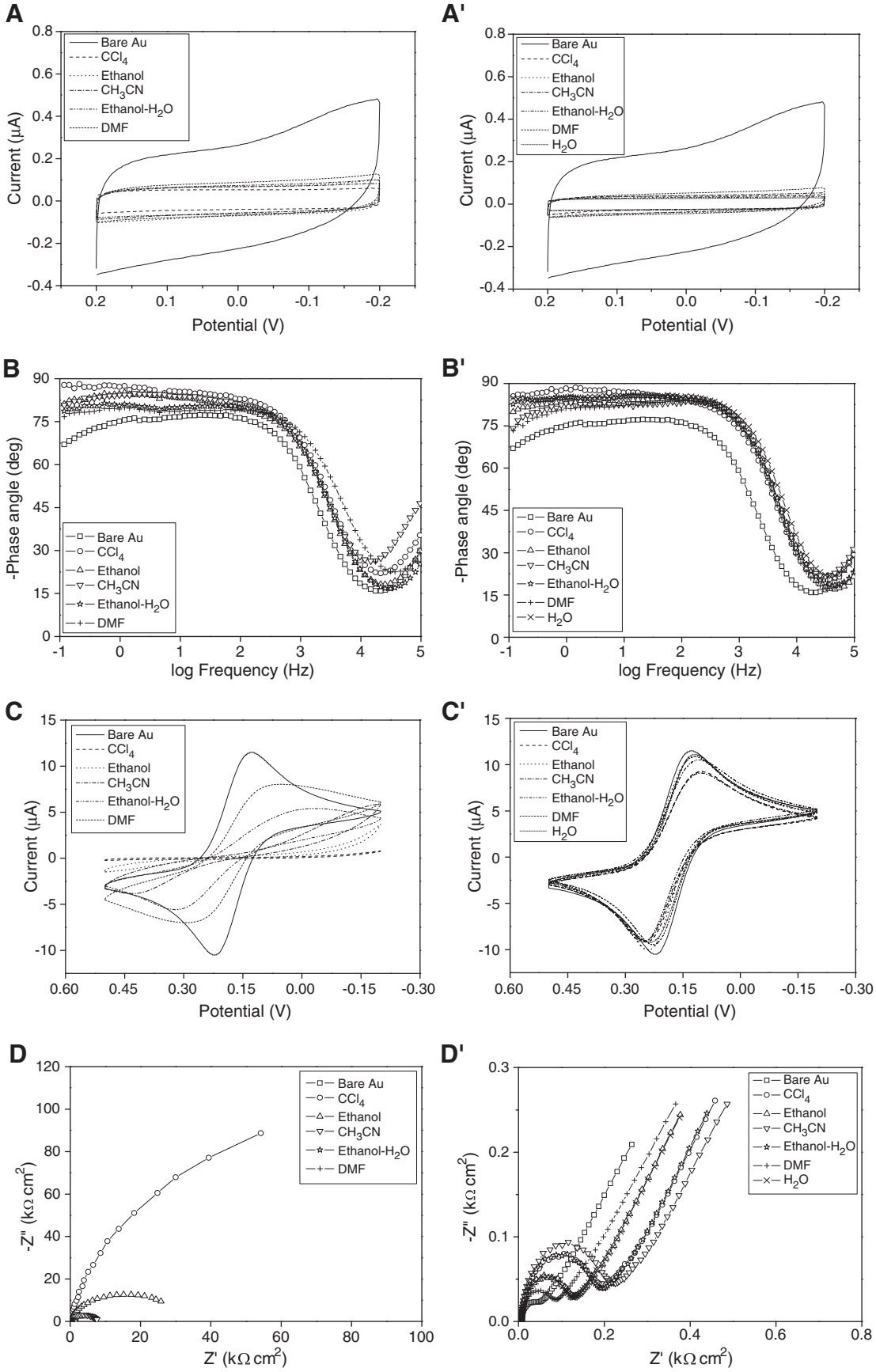

Fig. 3. Characteristics of TA-SAMs and MCH-SAMs on gold assembled in different solvents (because TA was nearly insoluble in H_2O, we investigated five solvents for assemble TA-SAMs and six solvents for assemble MCH-SAMs). (1) *CV* (scan rate, $v = 0.1\ V s^{-1}$) and *EIS* plots of bare Au and TA-SAMs (A and B) or MCH-SAMs (A′ and B′) in 0.1 M Na_2SO_4 solution. (2) *CV* (scan rate, $v = 0.1\ V s^{-1}$) and *EIS* plots of bare Au and TA-SAMs (C and D) or MCH-SAMs (C′ and D′) in 2 mM $K_3Fe(CN)_6$–0.1 M Na_2SO_4 solution.

Table 1
Interfacial parameters of TA-SAMs and MCH-SAMs on gold assembled in different solvents.

Thiols	Solvents	Ions permeability					$Fe(CN)_6^{3-}$ electron transfer	
		CV				*EIS*	*CV*	*EIS*
		C (μF cm^{-2})				$\Phi_{1\ Hz}$ (°)	Δi (μA cm^{-2})	R_{ct} (Ω cm^2)
		0.1 V s^{-1}	1 V s^{-1}	5 V s^{-1}	50 V s^{-1}			
TA	CCl_4	9.9 ± 0.2	8.8 ± 0.2	8.3 ± 0.6	7.1 ± 0.8	86 ± 2	22 ± 1	(2.4 ± 0.3) × 10^5
	Ethanol	15 ± 2	12 ± 1	11 ± 1	9.0 ± 0.5	84 ± 1	88 ± 34	(3.9 ± 1.2) × 10^4
	CH_3CN	14 ± 1	12 ± 1	11 ± 0	8.4 ± 0.3	84 ± 1	209 ± 21	(6.7 ± 1.0) × 10^3
	Ethanol–H_2O (1:1)	14 ± 1	12 ± 0	10 ± 1	7.9 ± 1.2	82 ± 2	243 ± 26	(1.0 ± 0.3) × 10^3
	DMF	18 ± 2	14 ± 2	12 ± 2	9.8 ± 2.2	82 ± 2	380 ± 56	(2.0 ± 1.3) × 10^2
Ref.	–	–	–	11 ± 3[a]	–	–	–	–
MCH	CCl_4	6.9 ± 0.5	6.1 ± 0.5	5.4 ± 0.2	4.9 ± 0.2	85 ± 2	451 ± 98	(1.3 ± 0.9) × 10^2
	Ethanol	9.2 ± 1.5	7.9 ± 1.4	7.0 ± 1.2	5.8 ± 0.8	84 ± 2	436 ± 57	(1.6 ± 1.2) × 10^2
	CH_3CN	8.9 ± 1.9	6.8 ± 0.9	6.0 ± 0.5	4.8 ± 0.1	82 ± 3	413 ± 23	(1.4 ± 0.6) × 10^2
	Ethanol–H_2O (1:1)	6.2 ± 0.1	5.7 ± 0.1	5.0 ± 0.1	4.4 ± 0.1	85 ± 1	382 ± 31	(2.1 ± 0.3) × 10^2
	DMF	11 ± 1	8.7 ± 0.9	7.6 ± 0.6	6.0 ± 0.3	82 ± 1	403 ± 27	(0.9 ± 0.1) × 10^2
	H_2O	5.5 ± 0.4	5.0 ± 0.2	4.6 ± 0.1	4.1 ± 0.2	85 ± 1	420 ± 18	(1.1 ± 0.1) × 10^2
Ref.	–	–	–	–	3.7[b]	–	–	–

(a) TA-SAMs assembled in 0.1% ethanolic solution for time (>24 h) [54,55]. (b) MCH-SAMs assembled in pure MCH for 30 min [25]. * Parameters of TA-SAMs and MCH-SAMs assembled in different solvents for 24 h were the average values of triplicate measurements (n=3) with relative standard deviation (RSD).

and R_{ct} (2.4 ± 0.3) × 10^5 Ω cm^2. TA-SAMs formed in ethanol/H_2O and DMF showed the poorer blocking to $Fe(CN)_6^{3-}$ electron transfer with Δi 243 ± 26 μA cm^{-2} (ethanol–H_2O) and 380 ± 56 μA cm^{-2} (DMF) as well as R_{ct} (1.0 ± 0.3) × 10^3 Ω cm^2 (ethanol–H_2O) and (2.0 ± 1.3) × 10^2 Ω cm^2 (DMF). Based on *C*, $\Phi_{1\ Hz}$, Δi and R_{ct}, the ability of solvents availing the ordering of TA-SAMs was CCl_4>ethanol>CH_3CN>ethanol–H_2O>DMF.

3.1.2. MCH-SAMs

Fig. 3(A′, B′, C′, D′) showed the *CV* and *EIS* plots of bare Au and MCH-SAMs. Charging current of MCH-SAMs formed in H_2O was the smallest and in DMF the biggest (Fig. 3A′). $\Phi_{1\ Hz}$ of MCH-SAMs formed in H_2O was the biggest (85 ± 1°) and the smallest (82 ± 1°) in DMF (Fig. 3B′). MCH-SAMs formed in all solvents showed the poor blocking

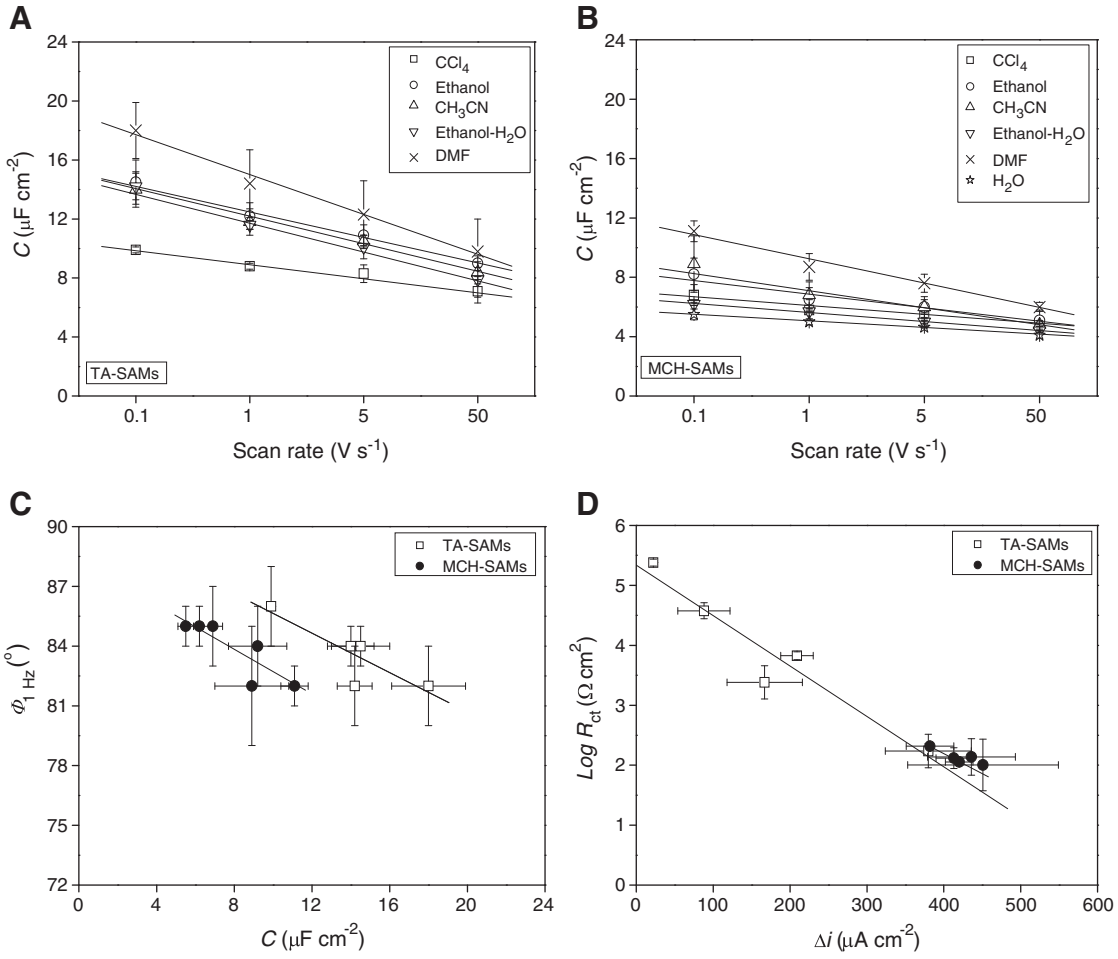

Fig. 4. The plots of *C* (A, TA-SAMs and B, MCH-SAMs) with scan rate *v*; the plots of $\Phi_{1\ Hz}$ with *C* obtained at 0.1 V s^{-1} (C) and logR_{ct} with Δi (D) of SAMs (TA and MCH) assembled in different solvents.

to $Fe(CN)_6^{3-}$ electron transfer with the almost same Δi ($414 \pm 48\ \mu A\ cm^{-2}$) and R_{ct} ($137 \pm 57\ \Omega\ cm^2$) (Fig. 3C′ and D′). Thus, the ability of solvents availing the ordering of MCH-SAMs was H_2O > ethanol–$H_2O \approx CCl_4$ > ethanol $\approx CH_3CN$ > DMF.

3.2. Relationships of C~v, $\Phi_{1\ Hz}$~C and Δi~logR_{ct} for TA-SAMs and MCH-SAMs

3.2.1. TA-SAMs

Fig. 4A showed the plots of C for TA-SAMs formed in different solvents with scan rate (v). C decreased with the increase of v, which reflected ions permeation in SAMs [7–12]. Cheng et al. obtained that C of TA-SAMs assembled in ethanolic solution was $11 \pm 3\ \mu F\ cm^{-2}$ (calculated at $v = 5.12\ V\ s^{-1}$) [54,55], consistent with our experimental value. The relationships of $\Phi_{1\ Hz}$ with C (calculated at $v = 0.1\ V\ s^{-1}$) and Δi with logR_{ct} were linear (Fig. 4C and D) with equations as:

$$\Phi_{1Hz}(^o) = 91 - 0.50\,C\left(\mu F\ cm^{-2}\right)\left(R^2 = 0.724\right)$$

$$\log R_{ct}\left(\Omega\ cm^2\right) = 5.3 - 8.4 \times 10^{-3}\Delta i(\mu A\ cm^{-2})\left(R^2 = 0.925\right)$$

3.2.2. MCH-SAMs

Fig. 4B showed the plots of C for MCH-SAMs formed in different solvents with v. The C~v plots indicated that ions permeation became serious at lower v. Miller et al. [25] assembled MCH with H_2O and ethanol as solvents and obtained that C was $3.7\ \mu F\ cm^{-2}$ ($v = 51.2\ V\ s^{-1}$) formed in aqueous solution and doubled formed in ethanolic solution, consistent with our experimental results. The relationships of $\Phi_{1\ Hz}$ with C (calculated at $v = 0.1\ V\ s^{-1}$) and Δi with logR_{ct} were linear (Fig. 4C and D) with equations as:

$$\Phi_{1Hz}(^o) = 88 - 0.56\,C\left(\mu F\ cm^{-2}\right)\left(R^2 = 0.920\right)$$

$$\log R_{ct}\left(\Omega\ cm^2\right) = 3.8 - 4.0 \times 10^{-3}\Delta i(\mu A\ cm^{-2})(R^2 = 0.758)$$

Recently, we [57] investigated the relationships of $\Phi_{1\ Hz}$ with C and logR_{ct} with Δi for TA-SAMs and MCH-SAMs assembled in thiols ethanolic solution for different times and obtained that the plots of $\Phi_{1\ Hz}$ with C and logR_{ct} with Δi were also linear. For TA-SAMs, $\Phi_{1\ Hz}$ (^{o}) = 96–0.88 C ($\mu F\ cm^{-2}$) ($R^2 = 0.863$) and logR_{ct} ($\Omega\ cm^2$) = 5.2-$7.9 \times 10^{-3}\ \Delta i$ ($\mu A\ cm^{-2}$) ($R^2 = 0.972$); for MCH-SAMs, $\Phi_{1\ Hz}$ (^{o}) = 93–1.1 C ($\mu F\ cm^{-2}$) ($R^2 = 0.886$) and logR_{ct} ($\Omega\ cm^2$) = $3.9–4.1 \times 10^{-3}\ \Delta i$ ($\mu A\ cm^{-2}$) ($R^2 = 0.846$) [57]. Comparing the equations with those obtained in this article, the linear equations (logR_{ct}~Δi) were almost the same, whereas the linear equations ($\Phi_{1\ Hz}$~C) presented the difference especially for the linear slopes. The smaller slopes for $\Phi_{1\ Hz}$~C in this article were perhaps due to the less sample data to obtain the fitting lines.

For the same thiols (TA or MCH), C obtained at low v ($0.1\ V\ s^{-1}$) had a big difference and was close to one another at high v ($50\ V\ s^{-1}$) (Fig. 4A and B). Considering the linear relationship of C ($0.1\ V\ s^{-1}$) with $\Phi_{1\ Hz}$, it indicated that C obtained at lower v had the similar meaning as $\Phi_{1\ Hz}$ (lower frequency) and could conveniently and roughly characterize ions permeability in SAMs. The C~v plots for C_{12}SH-SAMs reported [7,9,12] by us also proved the above conclusion. For different thiols, $\Phi_{1\ Hz}$ and C were not correlative and SAMs with bigger C did not indicate smaller $\Phi_{1\ Hz}$. Experimental results ($\Phi_{1\ Hz}$ with C) of $HS(CH_2)_{n-1}CH_3$-SAMs (n = 8, 10, 12, 16) reported by Boubour and Lennox [58] also accorded with the above conclusion. The reason was that $\Phi_{1\ Hz}$ only reflected ions permeation in SAMs [50,58,59], whereas C was related to the magnitude of both average dielectric constant and dielectric thickness in the interfacial region of SAMs [54,55].

Δi and R_{ct} were more sensitive to surface structure of TA-SAMs than MCH-SAMs. Because of the electrostatic repulsion between terminal —COO^- of TA ($pK_a = 6.5$) and $Fe(CN)_6^{3-}$ [60], $Fe(CN)_6^{3-}$ was hard to permeate into TA-SAMs and arrive at the gold surface, then the magnitude of Δi and R_{ct} reflected the collapsed sites in TA-SAMs [52,61] and surface arrangement of terminal —COO^-. Therefore, subtle differences in structural characteristics of TA-SAMs could be discerned. For MCH-SAMs, Δi and R_{ct} were almost independent of assembly solvents. Obvious redox peaks of $Fe(CN)_6^{3-}$ appeared showing that $Fe(CN)_6^{3-}$ could diffuse to the gold surface due to the lacking of electrostatic repulsion (—OH, $pK_a > 12$) [62] and defective surface structure of MCH-SAMs. The magnitude of Δi and R_{ct} reflected the defects (pinholes) [63] in MCH-SAMs. The diffusive layers of $Fe(CN)_6^{3-}$ redox reaction at defects could overlap which led to the almost constant Δi with R_{ct}. The same electrochemical response of redox probes on short-chain SAMs and bare Au surface from literature [54,55,64] also reflected the overlap of diffusive layers.

3.3. Exploration of the effect of solvents on self-assembly of thiols with different terminal groups on gold

Table 2 listed the parameters of solvents (E_T^N, δ and logP_{ow}) [65–68]. We drew the plots (Figs. 5 and 6) of electrochemical parameters (C, $\Phi_{1\ Hz}$, Δi and R_{ct}) of SAMs with E_T^N, δ and logP_{ow}. The changing tendencies of the plots of C and Δi with parameters of solvents were contrary to those of $\Phi_{1\ Hz}$ and R_{ct}. The fitting equations of the plots were listed below Figs. 5 and 6. Most of the equations could be expressed by the $y = a + b\ x + c\ x^2$ and $y = a + b\ x$, where y were the electrochemical parameters (C, $\Phi_{1\ Hz}$, Δi and R_{ct}), x were the parameters of solvents (E_T^N, δ and logP_{ow}) and a, b, c were the constants. It was difficult to give the physical meanings of the constants (a, b, c) only from the fitting equations for the two thiols, but we considered that this might provide the useful information for theoretically discussing the effect of solvents on thiols self-assembly on gold quantitatively based on the correlation of electrochemical parameters (C, $\Phi_{1\ Hz}$, Δi and R_{ct}) with parameters of solvents (E_T^N, δ and logP_{ow}). More thiols (especially a series of similar thiols, such as $HS(CH_2)_{n-1}CH_3$, $HS(CH_2)_{n-1}OH$ or $HS(CH_2)_{n-1}COOH$) should be chosen to study the relationships, define the physical meanings of fitting parameters and theoretically discuss the internal rules in the future.

For TA, C with Δi increased and $\Phi_{1\ Hz}$ with R_{ct} decreased with the decrease of logP_{ow} and the increase of E_T^N, δ on the whole (Fig. 5); For MCH, effect of solvents on MCH self-assembly was complex. C was much smaller and $\Phi_{1\ Hz}$ was much bigger when assembled in H_2O (the biggest E_T^N, δ and the smallest logP_{ow}) and CCl_4 (the smallest E_T^N, δ and the biggest logP_{ow}) than other solvents (Fig. 6A, B and C). Δi and R_{ct} were almost constant with the change of E_T^N, δ and logP_{ow} (Fig. 6A′, B′ and C′).

Table 2
Parameters of solvents (E_T^N, δ and logP_{ow}).

Solvents	E_T^N[a]	δ ($cal^{1/2}\ cm^{-3/2}$)[b]	logP_{ow}[c]	Solvent types
CCl_4	0.052	8.6	2.83	Nonpolar
DMF	0.386	12.1	−1.01	Polar aprotic
CH_3CN	0.460	11.9	−0.34	Polar aprotic
Ethanol	0.654	12.7	−0.30	Polar protic
Ethanol–H_2O[d]	0.827	18.1	−0.84	Polar protic
H_2O	1.000	23.4	−1.36	Polar protic

[a] E_T^N was defined as the overall soluble capability of solvents, which in turn depended on the action of all possible, nonspecific and specific, intermolecular interactions between solute ions or molecules and solvent molecules [65].

[b] δ was defined as the square root of the internal pressure or the cohesive energy density, and was a measurement of the intermolecular attractive forces [66].

[c] logP_{ow} was defined as the ratio of equilibrium concentration of a chemical in the octanol phase to that in the aqueous phase, and used to characterize quantitatively the hydrophobic nature of organic compounds. The bigger logP_{ow} was, the more hydrophobic solvent was [7,67,68].

[d] E_T^N, δ and logP_{ow} of ethanol–H_2O (1:1) calculated based on the volume ratio in the mixture [7].

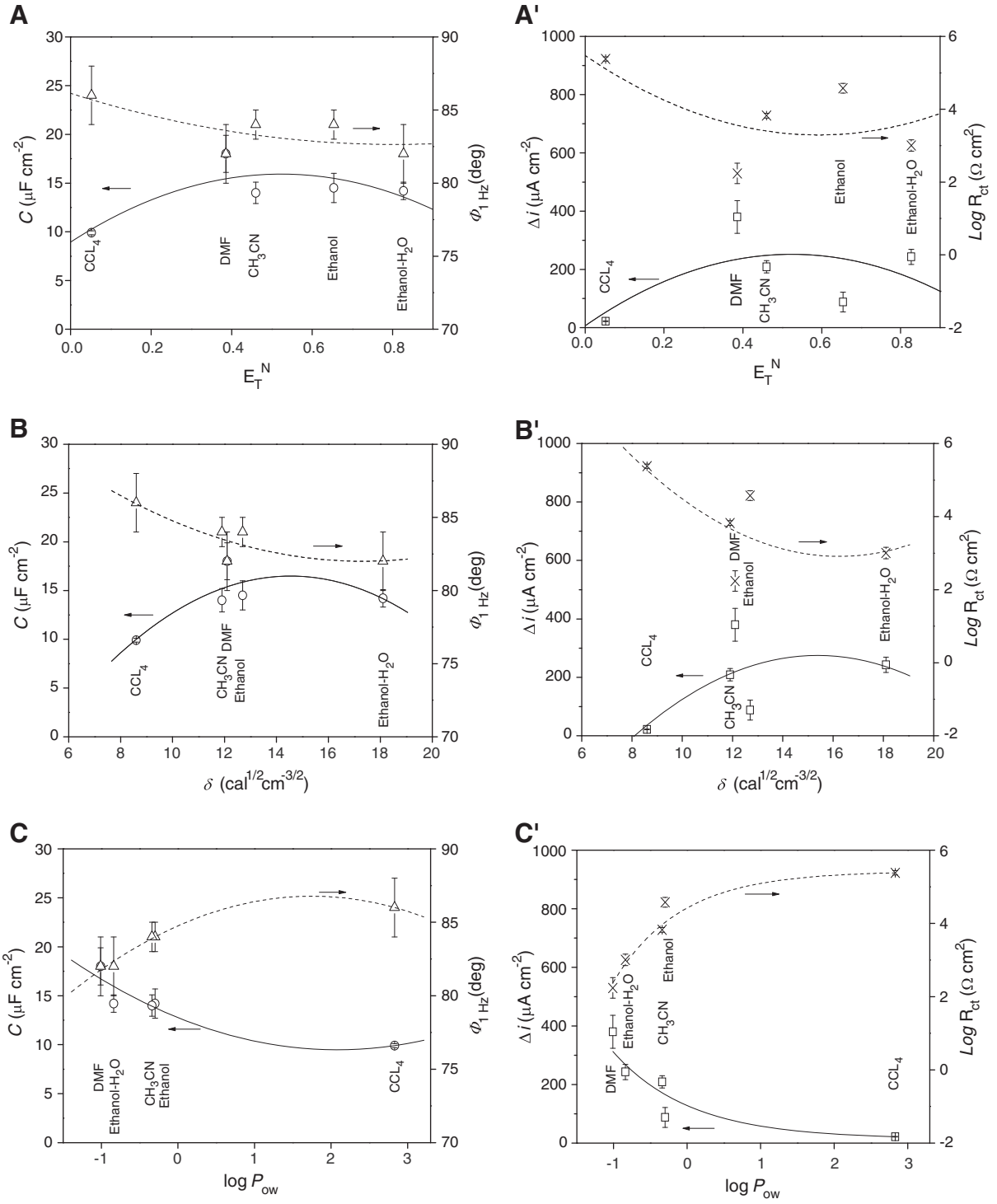

Fig. 5. Relationships of electrochemical parameters of TA-SAMs (C, Δi, $\Phi_{1\ Hz}$, R_{ct}) with parameters of solvents (E_T^N, δ, logP_{ow}). (C obtained at 0.1 V s^{-1} and $\Phi_{1\ Hz}$ were measured in 0.1 M Na_2SO_4 solution, whereas Δi and R_{ct} were measured in 2 mM $K_3Fe(CN)_6$–0.1 M Na_2SO_4 solution.) The fitting equations of the curves were:

(A) $C = 9.0 + 27E_T^N - 26E_T^{N_2}$ $\Phi_{1\ Hz} = 86 - 8.7E_T^N + 5.4E_T^{N_2}$

(A') $\Delta i = 6.4 + 938E_T^N - 896E_T^{N_2}$ $\log R_{ct} = 5.5 - 7.4E_T^N + 6.2E_T^{N_2}$

(B) $C = -22 + 5.4\delta - 0.18\delta^2$ $\Phi_{1\ Hz} = 98 - 1.8\delta - 0.052\delta^2$

(B') $\Delta i = -952 + 160\delta - 5.2\delta^2$ $\log R_{ct} = 14 - 1.3\delta - 0.040\delta^2$

(C) $C = 13 - 3.2\log P_{ow} - 0.76\log P_{ow}^2$ $\Phi_{1\ Hz} = 85 + 2.3\log P_{ow} - 0.66\log P_{ow}^2$

(C') $\Delta i = 14 + 114\exp(-\log P_{ow}/1.1)$ $\log R_{ct} = 5.4 - 1.0\exp(-\log P_{ow}/0.91)$.

We summarized the reports about the effect of solvents on thiol self-assembly on gold from literature (Table 3). For thiols with terminal group (—CH_3), solvents with bigger E_T^N and δ (smaller logP_{ow}) availed the ordering of SAMs, which was proved by our recent study about $C_{12}SH$ [7] and the experiments from other research groups [16,30,32,69–71]. For thiols with terminal group (—COOH), literature [26,29] reported that solvents with smaller E_T^N and δ (bigger logP_{ow}) availed the ordering of SAMs, which was consistent with our

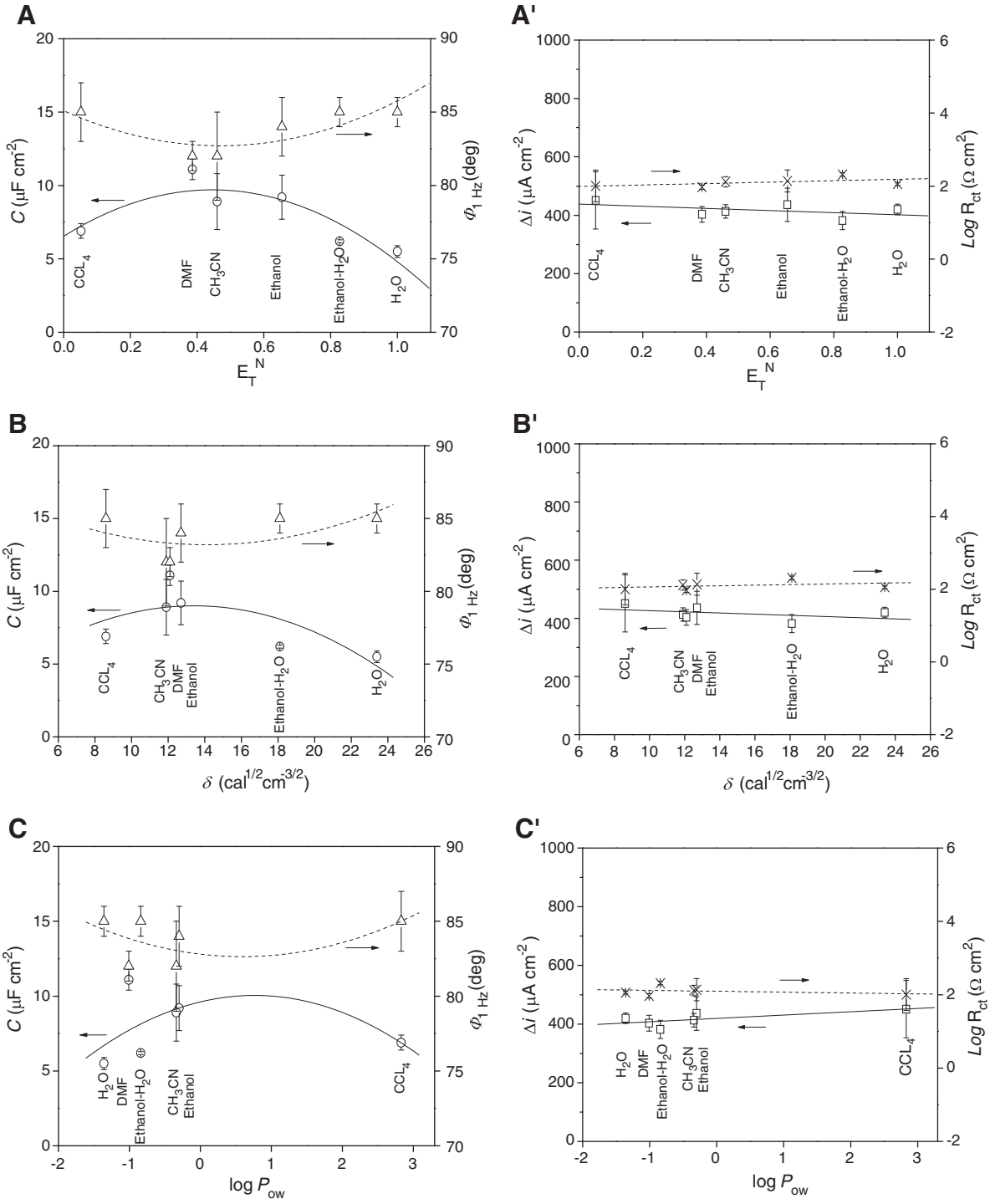

Fig. 6. Relationships of electrochemical parameters of MCH-SAMs (C, Δi, $\Phi_{1\ Hz}$, R_{ct}) with parameters of solvents (E_T^N, δ, logP_{ow}). (C obtained at 0.1 V s^{-1} and $\Phi_{1\ Hz}$ were measured in 0.1 M Na_2SO_4 solution, whereas Δi and R_{ct} were measured in 2 mM $K_3Fe(CN)_6$–0.1 M Na_2SO_4 solution.) The fitting equations of the curves were:

(A) $C = 6.5 + 14E_T^N - 16E_T^{N_2}$ $\Phi_{1\ Hz} = 85 - 10E_T^N + 11E_T^{N_2}$

(A') $\Delta i = 438 - 36E_T^N$ $\log R_{ct} = 2.0 - 0.20E_T^N$

(B) $C = 1.5 + 1.1\delta - 0.042\delta^2$ $\Phi_{1\ Hz} = 89 - 0.75\delta + 0.027\delta^2$

(B') $\Delta i = 447 - 2.0\delta$ $\log R_{ct} = 2.0 - 0.0080\delta$

(C) $C = 9.6 + 1.1\log P_{ow} - 0.74\log P_{ow}^2$ $\Phi_{1\ Hz} = 83 - 0.56\log P_{ow} + 0.47\log P_{ow}^2$

(C') $\Delta i = 419 + 11\log P_{ow}/1.1)$ $\log R_{ct} = 2.1 - 0.024\ \log P_{ow})$.

conclusion of TA self-assembly (Fig. 5) and contrary to the self-assembly of thiols (—CH_3). Furthermore, some literature indicated that proticity of —COOH was important in SAMs ordering [14,15,20,21]. For thiols with terminal group (—OH), there were few reports. Miller et al. [25] obtained that hydroxyl thiol-SAMs formed in H_2O were more compacted than in ethanol, accordant with our experimental conclusion about MCH self-assembly (Fig. 6).

It was anticipated that solvents with smaller E_T^N and δ (bigger logP_{ow}) did not favor the compactness of alkanethiol SAMs because they could soluble the alkane chains of thiols much more [7,18,32,71].

Table 3
Self-assembly of thiols on gold in different solvents from literature.

No.	Thiols	Solvents	Methods	Characteristics
1	Cysteamine (CA) Propanethiol (PT)	Toluene, ethanol, DMF and H_2O	STM	Proticity of solvent prior to the polarity determined the structure of CA-SAMs. Size of pits in PT-SAMs increased with decreasing the polarity of solvent except in DMF [28].
2	3-mercaptopropionic acid (MPA)	Chloroform and ethanol	SEIRAS	SAMs formed in chloroform were arranged to more normal direction than in e thanol against the gold surface [26].
3	Thioctic acid (TA)	Ethanol and ethanol–5% acetic acid	NEXAFS, XPS	SAMs formed in ethanol were highly disordered. Adding acetic acid to ethanol for assembly availed the formation of ordered TA-SAMs [20].
4	$HS(CH_2)_{n-1}OH$ (n = 3~17)	Ethanol and H_2O	CV	SAMs assembled with H_2O as solvent were much more compacted than with ethanol [25].
5	Mercaptohexanoic acid (MHA)	Ethanol, DMF, and H_2O	STM, CA	SAMs prepared with a polar aprotic solvent formed a more well-ordered structure and better hydrophilic surface than with a polar protic solvent [29].
6	$HSCH_2(CH_3)_3$	Tetrahydrofuran, ethanol, ethanol–H_2O (1:1), and H_2O	STM, CV	SAMs assembled with H_2O as solvent had the highest order [16].
7	$HS(CH_2)_9CH_3$	Heptane, toluene, ethanol, and DMF	STM	The assembly solvents affected the sizes of domains and pit sizes of SAMs formed. For SAMs formed in ethanol, flat regions corresponding to the SAM layer with the $(\sqrt{3}\times\sqrt{3})$ R30° structure and many pits were observed. For SAMs formed in DMF, pits were connected each other and the density of missing-row-defect was very low with big domains; for SAMs formed in toluene, the area of each pit seemed to be larger. For SAMs formed in heptane, SAMs were disordered and no clear flat regions appeared on gold surface [30].
8	$HS(CH_2)_{11}CH_3$	CCl_4, toluene, tetrahydrofuran, acetone, DMF, CH_3CN, ethanol, and ethanol–H_2O (1:1)	CV, EIS	High-quality C_{12}SH-SAMs formed when assembled in solvents with high E_T^N, δ and low logP_{ow} [7].
9	$HS(CH_2)_{10}COOH$ $HS(CH_2)_{15}COOH$	Ethanol and ethanol–acetic acid	STM, XPS, CV, EIS	SAMs assembled in ethanol or ethanol–acetic acid had the same quality [15].
10	$HS(CH_2)_{15}COOH$	Ethanol and ethanol–5% acetic acid	NEXAFS	SAMs prepared in ethanol–5% acetic acid was much more compacted than in ethanol only [21].
11	$HS(CH_2)_{11}COOH$, $HS(CH_2)_{11}NH_2$	Ethanol, ethanol–2% CF_3COOH, and ethanol–3% $N(CH_2CH_3)_3$	XPS, AFM, CA	Compared with ethanol as solvent, $HS(CH_2)_{11}COOH$-SAMs were more ordered when assembled in ethanol–2% CF_3COOH and rinsed by 10% NH_4OH. Similarly, $HS(CH_2)_{11}NH_2$-SAMs were more ordered when assembled in ethanol–3% $N(CH_2CH_3)_3$ and rinsed by 10% CH_3COOH [14].
12	$HS(CH_2)_{15}CH_3$	Hexadecane, hexane, tolune, ethanol, chloroform, acetonitrile, and DMF	CV, EIS	SAMs were highly impermeable when assembled in solvents like hexane and chloroform, compared to those formed in solvents like ethanol, DMF, acetonitrile, hexadecane and toluene [17].
13	$HS(CH_2)_{17}CH_3$	Acetonitrile	SERS	Acetonitrile could permeate and be trapped in C_{18}SH-SAMs [31].
14	$HS(CH_2)_{n-1}CH_3$ (n = 8, 10, 12, 16, 18)	Surfactant, ethanol, and isooctane	CV, EIS, FTIR, RIR	SAMs were more ordered when assembled in surfactant than ethanol or isooctane [18,32,33].
15	$HS(CH_2)_{n-1}CH_3$ (n = 8, 10, 12, 16, 18)	Superfluid CO_2, ethanol, and superfluid CO_2–ethanol	EIS, RIR	SAMs were more ordered when assembled in superfluid CO_2 or superfluid CO_2–ethanol than only ethanol [34,35].
16	3-(4-pyridine-4-yl-phenyl)-propane-1-thiol (PyP3)	Ethanol, acetonitrile and KOH–ethanol	STM, Xps, PM-IRRAS, NEXAFS	The quality of the SAM was strongly dependent on the solvent. Gold corrosion happened by using pure ethanol to assemble SAMs. In contrast, highly ordered and densely packed SAMs formed in acetonitrile or a KOH–ethanol mixture [36].

Scanning tunneling microscopy (STM); surface-enhanced infrared adsorption spectroscopy (SEIRAS); near-edge X-ray adsorption fine structure spectroscopy (NEXAFS); X-ray photoelectron spectroscopy (XPS); contact angle determination (CA); cyclic voltammetry (CV); electrochemical impedance spectroscopy (EIS); atomic force spectroscopy (AFM); surface-enhanced Raman scattering (SERS); grazing angle Fourier transform infrared spectroscopy (FTIR); reflectance-absorption infrared spectroscopy (RIR); and polarization-modulated infrared reflection absorption spectroscopy (PM-IRRAS).

However, the effect of solvents on TA self-assembly was just in reverse to the above conclusion. Therefore, other factors but soluble ability of solvents might dominate the ordering of TA-SAMs. The difference of solvents on self-assembly of thiols (terminal groups, —COOH and —OH) with that (—CH_3) indicated that interactions (electrostatic force or hydrogen bond) of terminal groups themselves or terminal groups with solvent molecules perhaps dominated the packing of SAMs [19,20,25,29,72,73]. For TA, in polar solvents, —COOH of thiols easily dissociated to —COO^- and strong electrostatic repulsion of adjacent —COO^- made SAMs disordered [19]; in apolar solvents, hydrogen bond interaction of adjacent —COOH increased and between —COOH and solvents reduced both availed the ordering of SAMs [20,29]. Unlike TA, —OH of MCH could not dissociate in all solvents, then the ordering of SAMs ascribed to the cooperative effects such as solubility of solvents for thiol chains [7] and hydrogen bond of adjacent —OH of thiols or —OH with solvents [25,73].

4. Conclusions

In this paper we investigated the effect of solvents (CCl_4, DMF, CH_3CN, ethanol, ethanol–H_2O and H_2O) on self-assembly of TA and MCH on gold by *CV* and *EIS* based on the electrochemical parameters (C, $\Phi_{1\ Hz}$, Δi and R_{ct}). The main conclusions were as follows: (1) The ability of solvents availing the ordering of SAMs was CCl_4>ethanol>CH_3CN>ethanol–H_2O>DMF (for TA) and H_2O>ethanol–$H_2O\approx CCl_4$-ethanol$\approx CH_3CN$>DMF (for MCH); (2) Solvents with bigger logP_{ow} (smaller E_T^N and δ) availed the ordering of TA-SAMs; effect of solvents on MCH self-assembly was complex and MCH-SAMs formed in H_2O (the biggest E_T^N, δ and the smallest logP_{ow}) and CCl_4 (the smallest E_T^N, δ and the biggest logP_{ow}) were more ordered than in other solvents; (3) Functional groups (—COOH and —OH) of thiols might play an important role in SAMs ordering due to the existence of electrostatic force or hydrogen bond of adjacent thiols or thiols with solvent molecules; (4) It was simple and convenient to judge the ordering of SAMs based on C, $\Phi_{1\ Hz}$, Δi and R_{ct} from *CV* and *EIS* as compared with other techniques (Table 3). Relating the electrochemical parameters with parameters of solvents by fitting equations might provide the useful information for theoretically discussing the effect of solvents on thiols self-assembly on gold in the future. This work made a useful supplement for exploring the effect of solvent on thiols self-assembly on gold. It was important to choose appropriate solvent to assemble thiols in order to optimize the surface properties of SAMs for practical application [15,27,38,74]. Investigation of the relationships of SAMs with assembly solvents and discussion of the internal rule were the task to be solved in the future [1].

Acknowledgments

This work is supported by the NSFC (nos. 20975049 and 20575025), State Key Laboratory of Electrochemistry of China in Changchun Applied Chemistry Institute (2008008) and the Analytical Center of Nanjing University.

References

[1] J.C. Love, L.A. Estroff, J.K. Kriebel, R.G. Nuzzo, G.M. Whitesides, Chem. Rev. 105 (2005) 1103.
[2] J.J. Gooding, F. Mearns, W.R. Yang, J.Q. Liu, Electroanalysis 15 (2003) 81.
[3] J.P. Collman, N.K. Devaraj, T.P.A. Eberspacher, C.E.D. Chidsey, Langmuir 22 (2006) 2457.
[4] R.L. Millen, J. Nordling, H.A. Bullen, M.D. Porter, Anal. Chem. 80 (2008) 7940.
[5] S. Stoycheva, M. Himmelhaus, J. Fick, A. Korniakov, M. Grunze, A. Ulman, Langmuir 22 (2006) 4170.
[6] R.M. Crooks, A.J. Ricco, Acc. Chem. Res. 31 (1998) 219.
[7] J.Y. Dai, Z.G. Li, J. Jin, J.J. Cheng, J. Kong, S.P. Bi, J. Electroanal. Chem. 624 (2008) 315.
[8] J.Y. Dai, J.J. Cheng, Z.G. Li, Y.Q. Shi, N. An, S.P. Bi, Electrochem. Commun. 10 (2008) 582.
[9] J.Y. Dai, J.J. Cheng, J. Jin, Z.G. Li, J. Kong, S.P. Bi, Electrochem. Commun. 10 (2008) 587.
[10] J.Y. Dai, J.J. Cheng, Z.G. Li, J. Jin, S.P. Bi, Electrochim. Acta 53 (2008) 3479.
[11] J.J. Cheng, J.Y. Dai, J. Jin, L. Qiu, G.Y. Fang, Z.G. Li, Y.B. Sun, S.P. Bi, Thin Solid Films 517 (2009) 3661.
[12] J.Y. Dai, Z.G. Li, J. Jin, Y.Q. Shi, J.J. Cheng, J. Kong, S.P. Bi, Biosens. Bioelectron. 24 (2009) 1074.
[13] L. Cheng, J.P. Yang, Y.X. Yao, D.W. Price, S.M. Dirk, J.M. Tour, Langmuir 20 (2004) 1335.
[14] H. Wang, S.F. Chen, L.Y. Li, S.Y. Jiang, Langmuir 21 (2005) 2633.
[15] S.M. Mendoza, I. Arfaoui, S. Zanarini, F. Paolucci, P. Rudolf, Langmuir 23 (2007) 582.
[16] Q.J. Chi, J.D. Zhang, J. Ulstrup, J. Phys. Chem. B 110 (2006) 1102.
[17] U.K. Sur, V. Lakshminarayanan, J. Electroanal. Chem. 565 (2004) 343.
[18] V. Ganesh, V. Lakshminarayanan, Langmuir 22 (2006) 1561.
[19] C. Méthivier, B. Beccard, C.M. Pradier, Langmuir 19 (2003) 8807.
[20] T.M. Willey, A.L. Vance, C. Bostedt, T. van Buuren, R.W. Meulenberg, L.J. Terminello, C.S. Fadley, Langmuir 20 (2004) 4939.
[21] T.M. Willey, A.L. Vance, T. van Buuren, C. Bostedt, A.J. Nelson, L.J. Terminello, C.S. Fadley, Langmuir 20 (2004) 2746.
[22] D. Käfer, G. Witte, P. Cyganik, A. Terfort, C. Wöll, J. Am. Chem. Soc. 128 (2006) 1723.
[23] O. Dannenberger, J.J. Wolff, M. Buck, Langmuir 14 (1998) 4679.
[24] C.D. Bain, E.B. Troughton, Y.T. Tao, J. Evall, G.M. Whitesides, R.G. Nuzzo, J. Am. Chem. Soc. 111 (1989) 321.
[25] C. Miller, P. Cuendet, M. Graetzel, J. Phys. Chem. 95 (1991) 877.
[26] T. Imae, H. Torii, J. Phys. Chem. B 104 (2000) 9218.
[27] R. Arnold, W. Azzam, A. Terfort, C. Wöll, Langmuir 18 (2002) 3980.
[28] S.Y. Lee, J. Noh, M. Hara, H. Lee, Mol. Cryst. Liq. Cryst. 377 (2002) 177.
[29] J. Noh, K. Konno, E. Ito, M. Hara, Jpn. J. Appl. Phys. 44 (2005) 1052.
[30] R. Yamada, H. Sakai, K. Uosaki, Chem. Lett. 7 (1999) 667.
[31] A. Kudelski, P. Krysinski, J. Electroanal. Chem. 443 (1998) 5.
[32] D. Yan, J.A. Saunders, G.K. Jennings, Langmuir 16 (2000) 7562.
[33] D. Yan, J.A. Saunders, G.K. Jennings, Langmuir 19 (2003) 9290.
[34] R.D. Weinstein, D. Yan, G.K. Jennings, Ind. Eng. Chem. Res. 40 (2001) 2046.
[35] D. Yan, G.K. Jennings, R.D. Weinstein, Ind. Eng. Chem. Res. 41 (2002) 4528.
[36] C. Silien, M. Buck, G. Goretzki, D. Lahaye, N.R. Champness, T. Weidner, M. Zharnikov, Langmuir 25 (2009) 959.
[37] S. Subramanian, S. Sampath, Anal. Bioanal. Chem. 388 (2007) 135.
[38] P. Kalimuthu, S.A. John, Electrochem. Commun. 7 (2005) 1271.
[39] C.M. Whelan, J. Ghijsen, J.J. Pireaux, K. Maex, Thin Solid Films 464 (2004) 388.
[40] W. Limbut, P. Kanatharana, B. Mattiasson, P. Asawatreratanakul, P. Thavarungkul, Biosens. Bioelectron. 22 (2006) 233.
[41] V. Anandan, R. Gangadharan, G.G. Zhang, Sensors 9 (2009) 1295.
[42] R.K. Shervedani, S.A. Mozaffari, Anal. Chem. 78 (2006) 4957.
[43] J.J. Gooding, Electroanalysis 20 (2008) 573.
[44] T. Laaksonen, O. Pelliniemi, B.M. Quinn, J. Am. Chem. Soc. 128 (2006) 14341.
[45] R. Guo, D. Georganopoulou, S.W. Feldberg, R. Donkers, R.W. Murray, Anal. Chem. 77 (2005) 2662.
[46] A.M. Smith, M.W. Ducey Jr., M.E. Meyerhoff, Biosens. Bioelectron. 15 (2000) 183.
[47] A. Kick, M. Bönsch, K. Kummer, D.V. Vyalikh, S.L. Molodtsov, M. Mertig, J. Electron. Spectrosc. Relat. Phenom. 172 (2009) 36.
[48] A.W. Peterson, R.J. Heaton, R.M. Georgiadis, Nucleic Acid Res. 29 (2001) 5163.
[49] M. Dijksma, B. Kamp, J.C. Hoogvliet, W.P. van Bennekom, Langmuir 16 (2000) 3852.
[50] E. Boubour, R.B. Lennox, Langmuir 16 (2000) 4222.
[51] M.D. Porter, T.B. Bright, D.L. Allara, C.E.D. Chidsey, J. Am. Chem. Soc. 109 (1987) 3559.
[52] P. Diao, D.L. Jiang, X.L. Cui, D.P. Gu, R.T. Tong, B. Zhong, J. Electroanal. Chem. 464 (1999) 61.
[53] H.O. Finklea, D.A. Snider, J. Fedyk, E. Sabatani, Y. Gafni, I. Rubinstein, Langmuir 9 (1993) 3660.
[54] Q. Cheng, A. Brajter-Toth, Anal. Chem. 64 (1992) 1998.
[55] Q. Cheng, A. Brajter-Toth, Anal. Chem. 67 (1995) 2767.
[56] Y.F. Xing, S.J. O'Shea, S.F.Y. Li, J. Electroanal. Chem. 542 (2003) 7.
[57] Z.G. Li, T.X. Niu, Z.J. Zhang, S.P. Bi, Electrochim. Acta 55 (2010) 6907.
[58] E. Boubour, R.B. Lennox, Langmuir 16 (2000) 7464.
[59] I. Burgess, B. Seivewright, R.B. Lennox, Langmuir 22 (2006) 4420.
[60] Y. Wang, A.E. Kaifer, J. Phys. Chem. B 102 (1998) 9922.
[61] F.Y. Ma, R.B. Lennox, Langmuir 16 (2000) 6188.
[62] V. Dharuman, J.H. Hahn, Sens. Actuators B 127 (2007) 536.
[63] X.Q. Lu, H.Q. Yuan, G.F. Zuo, J.D. Yang, Thin Solid Films 516 (2008) 6476.
[64] S. Lingler, I. Rubinstein, W. Knoll, A. Offenhausser, Langmuir 13 (1997) 7085.
[65] C. Reichardt, Chem. Rev. 94 (1994) 2319.
[66] A.F.M. Barton, Chem. Rev. 75 (1975) 731.
[67] E.M. Duffy, W.L. Jorgensen, J. Am. Chem. Soc. 122 (2000) 2878.
[68] W. Eisfeld, G. Maurer, J. Phys. Chem. B 103 (1999) 5716.
[69] S. Subramanian, S. Sampath, J. Colloid Interf. Sci. 313 (2007) 64.
[70] U.K. Sur, V. Lakshminarayanan, J. Electroanal. Chem. 516 (2001) 31.
[71] M.R. Anderson, M.N. Evaniak, M.H. Zhang, Langmuir 12 (1996) 2327.
[72] O. Dannenberger, K. Weiss, H.J. Himmel, B. Jäger, M. Buck, C. Wöll, Thin Solid Films 307 (1997) 183.
[73] G. Papastavrou, S. Akari, Colloids Surf. A 164 (2000) 175.
[74] J. Bowen, M. Manickam, S.D. Evans, K. Critchley, K. Kendall, J.A. Preece, Thin Solid Films 516 (2008) 2987.